

Serveur Académique Lausannois SERVAL serval.unil.ch

Author Manuscript

Faculty of Biology and Medicine Publication

This paper has been peer-reviewed but does not include the final publisher proof-corrections or journal pagination.

Published in final edited form as:

Title: Hypoglycemia-activated GLUT2 neurons of the nucleus tractus solitarius stimulate vagal activity and glucagon secretion.

Authors: Lamy CM, Sanno H, Labouèbe G, Picard A, Magnan C, Chatton JY, Thorens B

Journal: Cell metabolism

Year: 2014 Mar 4

Issue: 19

Volume: 3

Pages: 527-38

DOI: [10.1016/j.cmet.2014.02.003](https://doi.org/10.1016/j.cmet.2014.02.003)

In the absence of a copyright statement, users should assume that standard copyright protection applies, unless the article contains an explicit statement to the contrary. In case of doubt, contact the journal publisher to verify the copyright status of an article.

Hypoglycemia-activated Glut2 Neurons of the Nucleus Tractus Solitarius Stimulate Vagal Activity and Glucagon Secretion

Christophe M Lamy^{1,4}, Hitomi Sanno², Gwenaël Labouèbe², Alexandre Picard², Christophe Magnan³, Jean-Yves Chatton¹, Bernard Thorens²

¹ Department of Fundamental Neurosciences, University of Lausanne, Switzerland

² Center for Integrative Genomics, University of Lausanne, Switzerland

³ CNRS-University Paris Diderot, 75205 Paris Cedex 13, France

⁴ Department of Medicine, University of Fribourg, Switzerland

Co-Corresponding authors:

Prof. Bernard Thorens
Center for Integrative Genomics
University of Lausanne
Bâtiment Génopode, CH-1015 Lausanne, Switzerland
Phone: +41 21 692 3981
Email: Bernard.Thorens@unil.ch

PD Dr. Jean-Yves Chatton
Department of Fundamental Neurosciences
University of Lausanne
Rue du Bugnon 9, CH-1015 Lausanne, Switzerland
Phone: +41 21 692 5106
Email: Jean-Yves.Chatton@unil.ch

Running title: Glut2 neurons control glucagon secretion

SUMMARY

Glucose-sensing neurons in the brainstem participate in the regulation of energy homeostasis but have been poorly characterized because of the lack of specific markers to identify them. Here we show that Glut2-expressing neurons of the nucleus of the tractus solitarius form a distinct population of hypoglycemia-activated neurons. Their response to low glucose is mediated by reduced intracellular glucose metabolism, increased AMP-activated protein kinase activity, and closure of leak K^+ channels. These are GABAergic neurons that send projections to the vagal motor nucleus. Light-induced stimulation of channelrhodospin-expressing Glut2-neurons *in vivo* led to increased parasympathetic nerve firing and glucagon secretion. Thus Glut2-neurons of the nucleus tractus solitarius link hypoglycemia detection to counterregulatory response. These results may help identify the cause of hypoglycemia associated autonomic failure, a major threat in the insulin treatment of diabetes.

HIGHLIGHTS

- Glucose transporter Glut2 defines a subpopulation of glucose-sensing neurons in NTS
- NTS Glut2 neurons are excited when glucose levels drop
- Glucose sensing involves leak K^+ channels, cellular glucose metabolism and AMPK
- Glut2 neurons are GABAergic cells controlling vagal output and glucagon secretion

INTRODUCTION

Feeding, energy expenditure, and glucose homeostasis are processes that are regulated by many signals reflecting the metabolic status of the organism. Nutrients, including glucose, lipids and amino acids, play a particularly important role in orchestrating these responses by directly controlling the secretion of hormones such as insulin and glucagon, and by modulating the activity of the autonomic nervous system to coordinate the adaptation of peripheral organs to changes in energy metabolism (Schwartz et al., 2000; Thorens, 2012).

Glucose-sensing neurons have been identified and classified in two major categories, glucose excited (GE) and glucose inhibited (GI), depending on the effect of extracellular glucose on their firing activity (Routh, 2002). There is evidence for a large diversity in the mechanisms of neuronal glucose-sensing and for their wide topographical distribution (Thorens, 2012). It is established that the hypothalamus and brainstem are important centers that integrate nutrient, hormonal and nervous signals controlling energy metabolism. Evidence has been provided that NPY and POMC neurons in arcuate nucleus (AN), MCH and orexin neurons of the lateral hypothalamus (LH), as well as a large number of neurons from the ventromedial hypothalamus (VMH) are glucose-responsive and may control adaptive responses to hypo- or hyperglycemia (Gonzalez et al., 2009; Kang et al., 2004; Parton et al., 2007). In the brainstem, the dorsal vagal complex (DVC), which consists in the area postrema (AP), the nucleus of the tractus solitarius (NTS), and the dorsal motor nucleus of the vagus (DMNX), also contains GE and GI neurons (Balfour et al., 2006; Balfour and Trapp, 2007). These neurons are involved in various glucoregulatory functions, including the stimulation of feeding and glucagon secretion in response to hypoglycemia and the increase of insulin secretion in response to hyperglycemia (Marty et al., 2005; Marty et al., 2007; Ritter et al., 2000). They also control gastric motility (Ferreira et al., 2001; Grill and Hayes, 2012). Although there is abundant evidence for the presence of glucose-sensing neurons in brainstem, the lack of specific markers hampers a clear identification of these cells and any further characterization of their molecular mechanisms of glucose detection, and of the neuronal circuits in which they are integrated.

In previous studies we reported that expression of the glucose transporter Glut2 in the brain is required for several glucoregulatory responses, including glucagon secretion (Marty et al., 2005), feeding (Bady et al., 2006), and thermoregulation (Mounien et al., 2010). Using a genetic

reporter system we showed that Glut2-expressing neurons were scattered in different hypothalamic nuclei, including the LH, VMH, paraventricular hypothalamus and the zona incerta (Mounien et al., 2010). In the AN, Glut2-expressing nerve terminals were found in contact with NPY and POMC neurons, which did not express themselves this gene. Glut2 neurons were also found in brainstem, in particular in the DVC. In this structure, neuroglucopenia activated c-fos expression in Glut2 cells, suggesting that they are GI neurons (Mounien et al., 2010). More recently, we showed that *Glut2* inactivation in the nervous system (NG2KO mice) led to suppressed regulation by glucose of the parasympathetic and sympathetic nerve activity. This caused impaired proliferation of beta-cells during the weaning period, reduced adult beta-cell mass, suppression of first phase insulin secretion, and progressive development of glucose intolerance. When NG2KO mice were fed a high fat diet, glucose intolerance developed faster and glucagon secretion became deregulated (Tarussio et al., 2014). Thus, Glut2-expressing cells in the nervous system are involved in the control by glucose of the autonomic nervous activity, which controls endocrine pancreas development and function. However, the specific role of Glut2-neuron subpopulations present in different hypothalamic and brainstem nuclei is not yet defined.

Here, we report the electrophysiological properties of Glut2-neurons of the NTS, which form a homogeneous population of GI neurons mechanistically dependent on intracellular glucose metabolism, AMP-Kinase and activation of a leak K^+ current. Furthermore, we find that these neurons are GABAergic interneurons sending projections to the DMNX. We show that when activated by optogenetic tools, they increase parasympathetic activity and stimulate glucagon secretion, thus defining a neuronal circuit linking hypoglycemia detection to counterregulatory response.

RESULTS

Glut2 Cells Are Glucose-Sensing Neurons Excited by Low Glucose Levels

To identify Glut2-expressing cells in brainstem, we crossed Glut2-Cre mice (Mounien et al., 2010) with a Rosa26tdTomato reporter line (Madisen et al., 2010). We observed clusters of tdTomato-positive (tdT+) cells in the NTS of resulting animals (**Figure 1A**). These cells were more frequently found in the caudal and dorsal aspects of the NTS, in agreement with existing reports on the anatomical localization of Glut2 cells in the brainstem (Arluison et al., 2004). They appeared as multipolar neurons with extensive projections in and outside from NTS (**Figure 1A**). We performed whole-cell patch-clamp recordings in acute brainstem slices to analyze their electrophysiological properties (**Figure 1A** and **Table S1**). TdT+ cells were not spontaneously active, however, they fired accommodating spike trains when stimulated by depolarizing current injection (**Figure 1B**). Single-cell RT-PCR (scRT-PCR) amplification performed on cytosols collected at the end of electrophysiological recordings detected expression of Glut2 in 67% of tdT+ cells (**Figure 1C**). The failure to detect Glut2 in every cell we attribute to the low levels of expression of this gene (Arluison et al., 2004) and the low sensitivity of scRT-PCR. Because of this and the absence of Glut2 detection in all tested tdT- cells (*not shown*), we concluded that the tdTomato reporter system selectively labeled Glut2-expressing cells.

We assessed whether Glut2 neurons sensed extracellular glucose level by recording their electrical properties while changing glucose concentration in the superfusion buffer. Switching from 5 to 0.5mM glucose produced a reversible increase in resting membrane potential (V_m) of 6.7 ± 1.0 mV ($p < 2 \times 10^{-5}$, $n=13$) and in input resistance (R_{input}) of 451 ± 75 M Ω ($p < 6 \times 10^{-5}$, $n=13$) (**Figure 1D-E**). This glucose response pattern was observed consistently in all the tdT+ cells we recorded ($n=25$). By contrast, neighboring tdT- neurons were unresponsive to a similar change in glucose concentration ($\Delta V_m = -0.2 \pm 0.4$ mV, $p > 0.53$, $n=5$; $\Delta R_{input} = -129 \pm 133$ M Ω , $p > 0.38$; $n=5$), indicating that this effect is specific to Glut2 cells (**Figure S1A-B**). The response of tdT+ neurons to glucose was not altered when experiments were repeated in the presence of inhibitors of synaptic transmission ($\Delta V_m = 5.5 \pm 1.0$ mV, $p < 0.0002$, $n=12$; $\Delta R_{input} = 395 \pm 79$ M Ω , $p < 0.0004$, $n=12$), demonstrating a cell-autonomous effect (**Figure 1D-E**).

To test the impact of glucose-dependent variations in resting membrane properties on cell excitability, we injected depolarizing current steps and plotted the observed firing rates as a function of injected current intensity (FI curve). Switching from 5mM to 0.5mM glucose increased the firing frequency for the same amount of current injected (**Figure 1F**), leading to an increase in the slope of the FI curve (FI gain) of 0.082 ± 0.020 Hz/pA ($p < 0.0025$, $n = 10$; **Figure 1F-G**). This increase in excitability was confirmed by a decrease in the minimal amount of current required to trigger action potentials (Rheobase) of 30.8 ± 9.4 pA ($p < 0.0073$, $n = 12$; **Figure 1G**). The absence of any glucose effect on single action potential and spike train properties (**Table S2**) indicated that changes in excitability were only due to alterations of passive membrane properties. Experiments performed in the presence of synaptic blockers yielded similar changes in FI gain (Δ FI gain = 0.141 ± 0.038 Hz/pA, $p < 0.0047$, $n = 10$) and rheobase (Δ Rheobase = -16.4 ± 5.7 pA, $p < 0.016$, $n = 12$) than without inhibitors (**Figure 1G**), confirming that lowering glucose increased cell excitability independently from neuronal network activity.

We further determined that passive membrane properties and indices of cell excitability (FI gain and rheobase) changed monotonically with intermediate glucose concentrations (**Figure 1H**). Thus, Glut2 neurons reliably detect glucose changes for typical concentrations found in brain extracellular medium (Dunn-Meynell et al., 2009; Silver and Erecinska, 1994).

To exclude that the whole-cell approach used so far could affect cell responses by altering the concentration of intracellular metabolites and other regulatory factors, we performed cell-attached recordings to monitor cell excitability without interfering with cell content. Action potential firing increased by 2.3 fold ($p < 0.0039$, $n = 6$) when glucose concentration was lowered from 5 to 0.5mM, in the presence of synaptic blockers (**Figure S1C-D**), ruling out any significant effect of the recording procedure on the response of Glut2 neurons to glucose.

Leak Potassium Channels Drive the Glucose Response of Glut2 Neurons

We further investigated ionic conductances underlying glucose-induced inhibition in Glut2 neurons. The cell depolarization paired with R_{input} increase under lowered glucose (**Figure 1D-E**), suggested a mechanism involving the closure of a conductance for hyperpolarizing ions. Under recording conditions used in these experiments, calculated equilibrium potential for main ion

species present indicated that only K^+ ($E_K=-101\text{mV}$) and Cl^- ($E_{Cl}=-75\text{mV}$) currents would reverse at more hyperpolarized values than the resting membrane potential. We therefore acquired current-voltage (IV) relationships at different glucose concentrations. Switching glucose from 5mM to 0.5mM resulted in a reversible decrease in the IV curve slope (**Figure 2A**), corresponding to an increase of $323\pm 68\text{ M}\Omega$ in R_{input} ($p<6.4\times 10^{-4}$, $n=12$) in agreement with the change measured by periodic current pulse injection during continuous voltage recordings. In addition, IV curves showed that whole-cell currents varied monotonically with glucose concentration with the same non-linear dependency than cell properties measured previously (**Figure S2A**). Net glucose-induced current was calculated as the difference between current values measured at 5mM and 0.5mM. IV curve of net glucose current showed a reversal potential of $-95.5\pm 2.0\text{mV}$, indicating a conductance selective for K^+ (**Figure 2A**). Moreover, this IV curve had an outward rectifying trend well described by the Goldman-Hodgkin-Katz (GHK) current equation (**Figure 2A**), which pointed to a leak K^+ channel (Burdakov et al., 2006). The kinetics of net glucose-induced currents during voltage steps, consisting in a fast activation and an absence of decay over time (**Figure 2A**), are further attributes in favor of a leak K^+ conductance (Burdakov et al., 2006). The shape of net glucose current IV curve clearly excluded a voltage-gated K^+ channel or an inward rectifying K^+ channel. Calcium-dependent K^+ channels were unlikely to contribute to glucose effect since no changes in AHP and spike frequency adaptation were observed (**Table S2**).

To confirm the nature of the conductance responsible for the glucose effect, we performed recordings using a pipette solution with elevated Cl^- in order to shift the calculated equilibrium potential of this ion to a value more depolarized than resting membrane potential ($E_{Cl}=0\text{mV}$). In this condition, if Cl^- channels were involved, their opening at 5mM glucose would lead to an excitatory effect while decreasing glucose would result in inhibition. Instead, switching from 5mM to 0.5mM glucose produced a depolarization ($\Delta V_m=9.8\pm 1.3\text{mV}$, $p<1.9\times 10^{-5}$, $n=11$; **Figure 2B,D**) and an increase in cell excitability ($\Delta FI\text{ gain}=0.132\pm 0.041\text{ Hz/pA}$, $p<0.0047$, $n=9$; $\Delta R_{\text{heobase}}=-51.9\pm 17.3\text{ pA}$, $p<0.016$, $n=9$; **Figure 2D**) similar to the ones obtained with low pipette Cl^- , supporting the sole implication of K^+ channels. Continuous recording of glucose-induced current with high intrapipette Cl^- in the presence of tetrodotoxin unveiled an outward current of $18.6\pm 4.5\text{ pA}$ consistent with the closure of a K^+ conductance (**Figure 2C**). In agreement with the implication of leak K^+ channels, net glucose-induced current displayed an

outward rectification and reversed at a similar value than with low Cl^- intracellular solution ($E_{\text{rev}}=-103.8\pm 3.6\text{mV}$, $p>0.066$; **Figure S2B**).

We also pharmacologically probed the ionic mechanism of glucose effect. Bath application of leak K^+ channel blocker quinine (200 μM) produced an increase in V_m ($\Delta V_m=12.4\pm 2.2\text{mV}$, $p<0.003$, $n=6$) and R_{input} ($\Delta R_{\text{input}}=506\pm 172\text{ M}\Omega$, $p<0.033$, $n=6$; **Figure 2E-F**) and an inward shift of the IV curve (**Figure S2C**) indicative of the closure of a hyperpolarizing resting conductance. The quinine-inhibited current, obtained by subtracting currents before and after quinine application, was outward rectifying, reversed at $-97.5\pm 2.8\text{mV}$ and was fitted by the GHK current equation ($r^2=0.98$) (**Figure S2C**), confirming the expression of functional leak K^+ channels by NTS Glut2 neurons at rest. Furthermore, quinine prevented electrophysiological changes induced by lowering glucose concentration, ($\Delta V_m=1.5\pm 1.2\text{mV}$, $p<0.27$; $\Delta R_{\text{input}}=72\pm 36\text{ M}\Omega$, $p<0.11$, $n=6$; **Figure 2E-F**), showing that leak K^+ channels are required for the glucose response.

Glucose Metabolism Is Required for Glucose Sensing by Glut2 Neurons

We next tested if changes in Glut2 neuron excitability depended on glucose metabolism. Superfusion of the metabolic inhibitor 2-deoxyglucose (2-DG, 10mM) in the presence of 5mM glucose induced an increase in V_m ($\Delta V_m=6.8\pm 1.1\text{mV}$, $p<0.003$, $n=5$) and R_{input} ($\Delta R_{\text{input}}=263\pm 76\text{ M}\Omega$, $p<0.026$, $n=5$; **Figure 3A-B**) that mimicked the changes in membrane properties observed when lowering extracellular glucose, indicating that integrity of glucose metabolic pathways is important for the effect of glucose on these neurons. We then tested whether superfusion of glucokinase competitive inhibitor D-glucosamine in the presence of high glucose would mimic the effect of glucoprivation on Glut2 neurons. D-glucosamine (10mM) produced similar changes on resting membrane properties than glucose depletion ($\Delta V_m=5.8\pm 1.0\text{mV}$, $p<0.0014$, $n=7$; $\Delta R_{\text{input}}=182\pm 53\text{ M}\Omega$, $p<0.014$, $n=7$; **Figure 3C-D**), showing that the glucose-induced inhibition of Glut2 neurons depends on intracellular processing of glucose. Studies on glucose sensing mechanisms in other brain areas have reported direct effects of glucose on cell membrane without involvement of glucose metabolism (Gonzalez et al., 2009; O'Malley et al., 2006). To investigate whether glucose had a similar action on Glut2 neurons in NTS, we performed whole-cell recordings with glucose present in the pipette. In this condition, where intracellular glucose

metabolism is rendered independent from extracellular supply, responses to changes in extracellular glucose were abolished ($\Delta V_m = -0.5 \pm 0.4 \text{ mV}$, $p > 0.22$, $n = 7$; $\Delta R_{\text{input}} = -11 \pm 19 \text{ M}\Omega$, $p > 0.59$, $n = 7$; **Figure 3E-F**). Nevertheless, adding D-glucosamine to these neurons still produced a glucoprivic pattern of membrane response ($\Delta V_m = 5.4 \pm 0.9 \text{ mV}$, $p < 0.0014$, $n = 6$; $\Delta R_{\text{input}} = 407 \pm 123 \text{ M}\Omega$, $p < 0.022$; $n = 6$; **Figure 3E-F**), indicating that the presence of glucose in the pipette did not result in a non-specific blunting of cell responsiveness. These experiments confirmed that glucose sensing mechanism requires cellular glucose uptake and catabolism.

Glucose Response Is Mediated by AMPK

We hypothesized, in agreement with former results, that glucose effect on Glut2 neurons is mediated by changes in cellular energy levels. Inducing a cellular ATP depletion by the superfusion on mitochondrial ATPase inhibitor Oligomycin ($12 \text{ }\mu\text{M}$) resulted in an increase in V_m ($\Delta V_m = 7.2 \pm 1.7 \text{ mV}$, $p < 0.006$, $n = 7$) and R_{input} ($\Delta R_{\text{input}} = 474 \pm 102.3 \text{ M}\Omega$, $p < 0.004$, $n = 7$; **Figure 4A-B**) similar to the changes in membrane properties produced by low glucose levels, suggesting that a decrease of ATP supply is the main signal driving the response to glucoprivation.

Because AMP-activated protein kinase (AMPK) is a key sensor of cellular energy levels activated by ATP depletion and it is known to play an important role in the central regulation of energy homeostasis (Lage et al., 2008), we looked at its implication in the response of Glut2 neurons to glucose. Bath application of AMPK activator AICAR ($500 \text{ }\mu\text{M}$) produced similar effects than glucoprivation ($\Delta V_m = 8.5 \pm 1.4 \text{ mV}$, $p < 0.001$; $\Delta R_{\text{input}} = 411 \pm 129 \text{ M}\Omega$, $p < 0.020$, $n = 7$; **Figure 4C-D**). In addition, AMPK inhibitor Compound C ($150 \text{ }\mu\text{M}$) reversed the response to low glucose ($\Delta V_m = -5.1 \pm 1.2 \text{ mV}$, $p < 0.006$; $\Delta R_{\text{input}} = -396 \pm 92 \text{ M}\Omega$, $p < 0.005$, $n = 7$) and blocked glucose-dependent changes ($\Delta V_m = -0.6 \pm 0.5 \text{ mV}$, $p < 0.3$; $\Delta R_{\text{input}} = 27 \pm 57 \text{ M}\Omega$, $p < 0.7$, $n = 7$; **Figure 4E-F**). Finally, we detected the expression of AMPK by immunohistochemistry in 67.9 % of NTS Glut2 neurons ($n = 109$, **Figure 4G**). Together, these results demonstrate that AMPK mediates glucose sensing in NTS Glut2 neurons.

NTS Glut2 Neurons Are Inhibitory Cells Projecting to DMNX

We then performed immunohistochemistry to determine the nature of the Glut2-expressing cells. We observed that GAD67, a marker of GABAergic inhibitory neurons, was expressed in 80% of tdT+ cells (n=110; **Figure 5A**). Glut2 neurons also frequently expressed parvalbumin (PV), a marker found in GABAergic cells subpopulations (**Figure 5B**). GABAergic projections from NTS were previously shown to drive DMNX responses to glycemic changes (Ferreira et al., 2001). To check whether NTS Glut2 neurons project to DMNX, we filled them with biocytin during whole-cell recording and post-processed slices to reveal axonal projections of recorded cells with confocal microscopy. Co-immunostaining for choline acetyltransferase (ChAT) was used to localize DMNX cholinergic cells. Biocytin-filled axons from some of the NTS tdTomato-positive neurons we recorded could be followed down to DMNX (**Figure 5C**), with axons showing enlargements reminiscent of axonal boutons in this area (**Figure 5C**). This suggests that NTS Glut2 neurons provide GABAergic input to DMNX.

NTS Glut2 Neurons Activate the Vagus and Glucagon Secretion In Vivo

We sought to determine the role of Glut2 neurons in vivo. Because Glut2 neurons respond to low glucose levels and project to vagal motor neurons, we reasoned they may affect vagal output and drive the counterregulatory response to hypoglycemia. To test this hypothesis we used an optogenetics approach. We crossed Glut2-Cre mice with a Rosa26ChR2-YFP reporter line (Madisen et al., 2012) to express channelrhodopsin (ChR2) in Glut2 neurons. We recorded these cells by whole-cell patch-clamp in acute NTS slices to check the efficiency of ChR2 expression (**Figure 6A**). Blue light illumination (473 nm) induced a reversible photocurrent and action potential firing (**Figure 6B** and **S3A**). When using pulsed (10ms) illumination, the frequency of both photocurrents and action potentials increased with that of light pulses (**Figure 6C** and **S3B-C**). In vivo optogenetic stimulations were performed in anesthetized mice while vagal activity was recorded. An optical fiber was positioned with a stereotaxic micromanipulator at the dorsal face of the NTS to deliver pulses of blue light (**Figure 6D**). Light stimulation induced a rapid increase of vagal firing rate in ChR2-expressing animals but not in Cre-/ChR2+ littermates ($p < 0.0001$, 2-way anova, n=6; **Figure 6E**). Blood glucagon levels, measured shortly after the end of the stimulation, were significantly higher in ChR2-expressing animals as compared to Cre-/ChR2+ controls (glucagon=105.0±31.7, n=7 vs. 326.5±66.1 pg/ml, n=6, $p < 0.009$; **Figure**

6F). No differences in basal glucagonemia existed between the 2 groups (glucagon= 135.0 ± 51.5 , $n=11$ vs. 143.4 ± 21.6 pg/ml, $n=10$, $p < 0.9$; **Figure 6F**). These data evidence a role for NTS Glut2 neurons in the control of the parasympathetic regulation of glucagon secretion.

DISCUSSION

Our results establish that expression of the glucose transporter isoform Glut2 identifies a homogenous glucose-sensing neuronal subpopulation in the nucleus of the tractus solitarius. These Glut2 neurons are glucose-inhibited cells whose response depends on intracellular glucose metabolism-driven changes in permeability of background potassium channels; they are GABAergic inhibitory neurons. Optogenetic activation of these NTS Glut2 neurons activates parasympathetic nerve firing and glucagon secretion, suggesting that they play an important role in the counterregulatory response to hypoglycemia.

Glucose-sensing neurons have been identified in several brain areas involved in the control of energy homeostasis and related behaviors (Thorens, 2012). In the dorsal vagal complex, about 20% of neurons respond to glucose with either a GE or a GI pattern (Balfour et al., 2006; Yettefti et al., 1997). GI neurons in this structure use a variety of molecular mechanisms to couple hypoglycemia to changes in membrane excitability (Balfour and Trapp, 2007), indicating that they form a diverse population of glucose-responsive cells. Their precise topographical and functional characterization is however difficult to assess because of the absence of specific markers allowing their identification. In this study, we found Glut2 to consistently single out a specific population of GI neurons in NTS. This glucose transporter isoform was first described for its role in glucose sensing in pancreatic beta-cells leading to insulin secretion. Previous data suggested that it might hold a similar role in central glucose detection (Marty et al., 2005; Mounien et al., 2010) and in the control by glucose of the parasympathetic and sympathetic nervous activities (Tarussio et al., 2014). Here we provide evidence for the functional association of Glut2 with glucose-sensing in neurons. Whole-cell and cell-attached recordings showed that lowering glucose increased excitability of Glut2-expressing neurons, an effect relying on glucose metabolism, and on the subsequent closure of leak K^+ channels. A mediator of this response is an increase in intracellular AMP/ATP ratio that activates AMP-kinase, as shown for the response of other GI neurons such as those of the VMH (Murphy et al., 2009).

Membrane depolarization of GI neurons has been attributed to diverse mechanisms, including the reduction of Na^+/K^+ ATPase activity (Balfour and Trapp, 2007), the AMP-kinase-dependent inhibition of the CFTR chloride conductance (Murphy et al., 2009), or the closure of leak K^+ channels (Balfour and Trapp, 2007; Burdakov et al., 2006). We show that NTS Glut2

neurons' response to low glucose depends on a leak K^+ channel. However, in contrast to NTS Glut2 neurons, leak K^+ channel-driven glucoprivic signaling in LH orexin neurons does not require glucose uptake or metabolism, but a putative cell surface receptor (Gonzalez et al., 2009). Thus, hypoglycemia can use different signaling pathways to control the same membrane conductances.

An important observation is that depolarization of Glut2 NTS neurons increased progressively as external glucose concentrations decreased below euglycemic-like levels, however within the physiological extracellular concentration range found in the brain. Thus, glucose-sensitive Glut2-expressing neurons are in a position to fine-tune NTS glucoregulatory responses over physiological glucose concentrations.

Numerous studies indicated that brainstem and NTS glucose-responsive neurons are involved in whole body glucoregulation, such as neuroglucopenia-induced counterregulation and stimulation of feeding (Briski and Marshall, 2000; Dunn-Meynell et al., 2009). It was also shown that NTS neurons were connected to pancreas-projecting DMNX neurons by retrograde labeling using pseudorabies viruses (Buijs et al., 2001). In addition, NTS stimulation evoked GABAergic synaptic activity in DMNX (Ferreira et al., 2001). Here we showed that optogenetic activation of GABAergic Glut2-neurons of the NTS led to increased activity of vagal nerve and glucagon secretion. Although it is not known whether optogenetic stimulation resumes *in vivo* activation patterns by hypoglycemia, these results strongly suggest that NTS Glut2 neurons participate to physiological glucoregulatory responses.

Activation of parasympathetic nerves by NTS GABA neurons is consistent, on the one hand, with our observation that NTS Glut2 neurons send projections into the DMNX and, on the other hand, with the demonstration that a sizeable fraction of the NTS GABAergic input to the DMNX activates vagal nerves through inhibition of local tonic inhibitory neurons (Babic et al., 2011). The fact that hypoglycemia-induced parasympathetic activity stimulates glucagon secretion is well established (Berthoud et al., 1990; Patel, 1984). Parasympathetic activity triggers the initial counterregulatory response to hypoglycemia when blood glucose concentration falls below euglycemia whereas activation of sympathetic activity is triggered at lower glycaemic levels (Taborsky and Munding, 2012). In previous studies we showed that hypoglycemia or 2-DG-induced neuroglucopenia induced differential glucagon secretion in

control and Glut2-null mice. Importantly, this differential response was observed at intermediate levels of hypoglycemia (2.5 mM) or following injections carefully selected doses of 2-DG. At lower glycaemic levels (1 mM) or following injection of larger doses of 2-DG glucagon secretion was equally stimulated in control and knockout mice (Burcelin and Thorens, 2001; Marty et al., 2005). We thus hypothesized that Glut2-dependent nervous glucose sensing was involved in the detection of small, physiological changes in glycaemic levels, while other mechanisms, such as a direct stimulation of pancreatic α cell secretion, might take place during deeper hypoglycemia (Zhang et al., 2013). Our present data showing that NTS Glut2 neurons are GI neurons inducing glucagon secretion through activation of parasympathetic activity is in agreement with this previous hypothesis.

Collectively, our study provides the functional characterization of a new class of glucose-sensing neurons based on the expression of the Glut2 glucose transporter. They demonstrate that the NTS is indeed an important site for glucose sensing, in particular during development of hypoglycemia, which can be mobilized to induce glucagon secretion. This is an important step in elucidating the mechanisms controlling stimulated glucagon secretion in physiological conditions but also when this secretion becomes unresponsive to developing hypoglycemia, as associated with hypoglycemia associated autonomic failure (Cryer, 2006), a serious condition that limits insulin treatment of both type 1 and type 2 diabetes.

EXPERIMENTAL PROCEDURES

Slice preparation

Sagittal slices of brainstem, 200 μ m thick, containing NTS were cut in ice-cold extracellular solution with 10mM glucose using a vibratome and were maintained in an incubation chamber at room temperature until used.

Electrophysiology

Slices were placed in a submerged-type recording chamber and continuously superfused with extracellular solution at room temperature. TdTomato-expressing neurons were localized by confocal epifluorescence microscopy. Whole-cell recordings from visually identified neurons were obtained with borosilicate glass pipettes. Continuous recordings of V_m were used to monitor the effect of glucose and drugs. Hyperpolarizing current pulses were periodically injected to monitor R_{input} . Step protocols were used for additional measurements of cell properties. Cell attached recordings were performed on slice superfused with an extracellular solution promoting spontaneous firing.

Data analysis

Electrophysiological data were analyzed with pClamp10 (Molecular Devices). Voltages were corrected for calculated liquid junction potentials. Pooled data were presented as mean \pm SEM. Statistical analysis and curve fitting were done with Origin8.5 (OriginLab). Statistical testing was performed with paired and unpaired 2-tailed Student's t tests unless stated otherwise. Differences were considered significant for $p < 0.05$ (* $p < 0.05$; ** $p < 0.01$; *** $p < 0.001$, n.s., non significant).

Single cell RT-PCR

The single-cell content was aspirated with a patch pipette and expelled into an RNase free PCR tube for reverse transcription. We then performed two successive PCR rounds. The first round used the cDNAs present in the reverse transcription reaction as template. The second round used 10 μ l of the first PCR product as template. The products of the second PCR round were analyzed on agarose gel using ethidium bromide.

Immunohistochemistry

Immunostaining were done on brainstem cryosections obtained from mice perfused with 4% paraformaldehyde. Sections were incubated with primary monoclonal antibodies against GAD67 (MAB5406, Chemicon), PV (PV235, Swant), pAMPK (ab2535, Cell Signaling) and with an anti-mouse FITC-coupled secondary antibody. To reveal biocytin-filled neurons, acute slices were fixed with PFA 4% after recording and incubated with Cascade Blue-Neutravidin (A2663, Invitrogen). In addition, immunostaining was performed on these slices with a monoclonal antibody against choline acetyltransferase (ab35948, Abcam).

Image acquisition and processing

Confocal images of immunostained cryosections and acute slices were obtained and processed with Image J (Rasband, W.S., NIH, Bethesda, Maryland, USA) to obtain maximum intensity projection representations. High resolution images were deconvolved with Huygens (Scientific Volume Imaging, Hilversum, The Netherlands). In addition, three-dimensional surface renderings were produced with Imaris (Bitplane, Zurich, Switzerland).

Optogenetics experiments

ChR2-expressing neurons were activated with a blue laser (473 nm, 100 mW, Rapp-Optoelectronics) coupled to an optical fiber (200 μ m core, Thorlabs). For slice experiments, the fiber was attached to a micromanipulator and brought close to the recorded cell. Blue light-induced photo-currents and action potentials were recorded. For in vivo experiments, the fiber was positioned above the NTS of anesthetized mice with a stereotaxic apparatus. Repetitive trains of blue light pulses were applied for 40 min. The firing rate of the vagus nerve was monitored during the stimulation. Blood glucagon levels were dosed by radioimmunoassay shortly after the end of the stimulation.

ACKNOWLEDGEMENTS

This work was supported by the Swiss National Science Foundation (Grants No.3100A0-113525 to B.T. and No.31003A-135720 to J.Y.C.) and an Advanced Research Grant from the European Research Council (INSIGHT) to B.T. Acquisition and processing of confocal images was done at the Cellular Imaging Facility of the University of Lausanne. We thank Dr Denis Burdakov for useful comments.

REFERENCES

- Arluison, M., Quignon, M., Nguyen, P., Thorens, B., Leloup, C., and Penicaud, L. (2004). Distribution and anatomical localization of the glucose transporter 2 (GLUT2) in the adult rat brain--an immunohistochemical study. *J. Chem. Neuroanat.* 28, 117-136.
- Babic, T., Browning, K.N., and Travagli, R.A. (2011). Differential organization of excitatory and inhibitory synapses within the rat dorsal vagal complex. *Am. J. Physiol. Gastrointest. Liver Physiol.* 300, G21-32.
- Bady, I., Marty, N., Dallaporta, M., Emery, M., Gyger, J., Tarussio, D., Foretz, M., and Thorens, B. (2006). Evidence from glut2-null mice that glucose is a critical physiological regulator of feeding. *Diabetes* 55, 988-995.
- Balfour, R.H., Hansen, A.M., and Trapp, S. (2006). Neuronal responses to transient hypoglycaemia in the dorsal vagal complex of the rat brainstem. *J. Physiol.* 570, 469-484.
- Balfour, R.H., and Trapp, S. (2007). Ionic currents underlying the response of rat dorsal vagal neurones to hypoglycaemia and chemical anoxia. *J. Physiol.* 579, 691-702.
- Berthoud, H.R., Fox, E.A., and Powley, T.L. (1990). Localization of vagal preganglionics that stimulate insulin and glucagon secretion. *Am J Physiol* 258, R160-168.
- Briski, K.P., and Marshall, E.S. (2000). Caudal brainstem Fos expression is restricted to periventricular catecholamine neuron-containing loci following intraventricular administration of 2-deoxy-D-glucose. *Exp. Brain Res.* 133, 547-551.
- Buijs, R.M., Chun, S.J., Nijijima, A., Romijn, H.J., and Nagai, K. (2001). Parasympathetic and sympathetic control of the pancreas: a role for the suprachiasmatic nucleus and other hypothalamic centers that are involved in the regulation of food intake. *J. Comp. Neurol.* 431, 405-423.
- Burcelin, R., and Thorens, B. (2001). Evidence that extrapancreatic GLUT2-dependent glucose sensors control glucagon secretion. *Diabetes* 50, 1282-1289.

Burdakov, D., Jensen, L.T., Alexopoulos, H., Williams, R.H., Fearon, I.M., O'Kelly, I., Gerasimenko, O., Fugger, L., and Verkhatsky, A. (2006). Tandem-pore K⁺ channels mediate inhibition of orexin neurons by glucose. *Neuron* 50, 711-722.

Cryer, P.E. (2006). Mechanisms of sympathoadrenal failure and hypoglycemia in diabetes. *J Clin Invest* 116, 1470-1473.

Dunn-Meynell, A.A., Sanders, N.M., Compton, D., Becker, T.C., Eiki, J., Zhang, B.B., and Levin, B.E. (2009). Relationship among brain and blood glucose levels and spontaneous and glucoprivic feeding. *J. Neurosci.* 29, 7015-7022.

Ferreira, M., Jr., Browning, K.N., Sahibzada, N., Verbalis, J.G., Gillis, R.A., and Travagli, R.A. (2001). Glucose effects on gastric motility and tone evoked from the rat dorsal vagal complex. *J. Physiol.* 536, 141-152.

Gonzalez, J.A., Reimann, F., and Burdakov, D. (2009). Dissociation between sensing and metabolism of glucose in sugar sensing neurones. *J. Physiol.* 587, 41-48.

Grill, H.J., and Hayes, M.R. (2012). Hindbrain neurons as an essential hub in the neuroanatomically distributed control of energy balance. *Cell Metab* 16, 296-309.

Kang, L., Routh, V.H., Kuzhikandathil, E.V., Gaspers, L.D., and Levin, B.E. (2004). Physiological and molecular characteristics of rat hypothalamic ventromedial nucleus glucosensing neurons. *Diabetes* 53, 549-559.

Lage, R., Dieguez, C., Vidal-Puig, A., and Lopez, M. (2008). AMPK: a metabolic gauge regulating whole-body energy homeostasis. *Trends Mol Med* 14, 539-549.

Madisen, L., Mao, T., Koch, H., Zhuo, J.M., Berenyi, A., Fujisawa, S., Hsu, Y.W., Garcia, A.J., 3rd, Gu, X., Zanella, S., Kidney, J., Gu, H., Mao, Y., Hooks, B.M., Boyden, E.S., Buzsaki, G., Ramirez, J.M., Jones, A.R., Svoboda, K., Han, X., Turner, E.E., and Zeng, H. (2012). A toolbox of Cre-dependent optogenetic transgenic mice for light-induced activation and silencing. *Nat Neurosci* 15, 793-802.

Madisen, L., Zwingman, T.A., Sunkin, S.M., Oh, S.W., Zariwala, H.A., Gu, H., Ng, L.L., Palmiter, R.D., Hawrylycz, M.J., Jones, A.R., Lein, E.S., and Zeng, H. (2010). A robust and high-throughput Cre reporting and characterization system for the whole mouse brain. *Nat. Neurosci.* 13, 133-140.

Marty, N., Dallaporta, M., Foretz, M., Emery, M., Tarussio, D., Bady, I., Binnert, C., Beermann, F., and Thorens, B. (2005). Regulation of glucagon secretion by glucose transporter type 2 (glut2) and astrocyte-dependent glucose sensors. *J. Clin. Invest.* 115, 3545-3553.

Marty, N., Dallaporta, M., and Thorens, B. (2007). Brain glucose sensing, counterregulation, and energy homeostasis. *Physiology (Bethesda)* 22, 241-251.

Mounien, L., Marty, N., Tarussio, D., Metref, S., Genoux, D., Preitner, F., Foretz, M., and Thorens, B. (2010). Glut2-dependent glucose-sensing controls thermoregulation by enhancing the leptin sensitivity of NPY and POMC neurons. *FASEB J.*

Murphy, B.A., Fakira, K.A., Song, Z., Beuve, A., and Routh, V.H. (2009). AMP-activated protein kinase and nitric oxide regulate the glucose sensitivity of ventromedial hypothalamic glucose-inhibited neurons. *Am J Physiol Cell Physiol* 297, C750-758.

O'Malley, D., Reimann, F., Simpson, A.K., and Gribble, F.M. (2006). Sodium-coupled glucose cotransporters contribute to hypothalamic glucose sensing. *Diabetes* 55, 3381-3386.

Parton, L.E., Ye, C.P., Coppari, R., Enriori, P.J., Choi, B., Zhang, C.Y., Xu, C., Vianna, C.R., Balthasar, N., Lee, C.E., Elmquist, J.K., Cowley, M.A., and Lowell, B.B. (2007). Glucose sensing by POMC neurons regulates glucose homeostasis and is impaired in obesity. *Nature* 449, 228-232.

Patel, D.G. (1984). Role of parasympathetic nervous system in glucagon response to insulin-induced hypoglycemia in normal and diabetic rats. *Metabolism* 33, 1123-1127.

Ritter, S., Dinh, T.T., and Zhang, Y. (2000). Localization of hindbrain glucoreceptive sites controlling food intake and blood glucose. *Brain Res.* 856, 37-47.

Routh, V.H. (2002). Glucose-sensing neurons: are they physiologically relevant? *Physiol. Behav.* 76, 403-413.

Schwartz, M.W., Woods, S.C., Porte, D., Jr., Seeley, R.J., and Baskin, D.G. (2000). Central nervous system control of food intake. *Nature* 404, 661-671.

Silver, I.A., and Erecinska, M. (1994). Extracellular glucose concentration in mammalian brain: continuous monitoring of changes during increased neuronal activity and upon limitation in oxygen supply in normo-, hypo-, and hyperglycemic animals. *J. Neurosci.* 14, 5068-5076.

Taborsky, G.J., Jr., and Mundinger, T.O. (2012). Minireview: The role of the autonomic nervous system in mediating the glucagon response to hypoglycemia. *Endocrinology* 153, 1055-1062.

Tarussio, D., Metref, S., Seyer, S., Mounien, L., Vallois, D., Magnan, C., Foretz, M., and Thorens, B. (2014). Nervous control of postnatal beta-cell proliferation and glucose homeostasis. *J Clin Invest.* 124, 413-424.

Thorens, B. (2012). Sensing of glucose in the brain. *Handb. Exp. Pharmacol.* 209, 277-294.

Yettefti, K., Orsini, J.C., and Perrin, J. (1997). Characteristics of glycemia-sensitive neurons in the nucleus tractus solitarii: possible involvement in nutritional regulation. *Physiol. Behav.* 61, 93-100.

Zhang, Q., Ramracheya, R., Lahmann, C., Tarasov, A., Bengtsson, M., Braha, O., Braun, M., Brereton, M., Collins, S., Galvanovskis, J., Gonzalez, A., Groschner, L.N., Rorsman, N.J., Salehi, A., Travers, M.E., Walker, J.N., Gloyn, A.L., Gribble, F., Johnson, P.R., Reimann, F., Ashcroft, F.M., and Rorsman, P. (2013). Role of KATP channels in glucose-regulated glucagon secretion and impaired counterregulation in type 2 diabetes. *Cell Metab* 18, 871-882.

FIGURE LEGENDS**Figure 1. Glucose Response of Glut2 Neurons in NTS**

(A) Confocal images of Glut2 neurons in NTS showing a cluster of td-Tomato labeled neurons (left) and a single neuron patched superimposed with the corresponding infrared DIC image in an acute mouse brainstem slice (right). Recording pipette is delineated by white dashed lines.

(B) Voltage trace from a Glut2 neuron showing a typical accommodating spike train induced by depolarizing current injection.

(C) Agarose gel showing RT-PCR amplification products of Glut2 and control gene β -actin from the cytosol of single tdTomato-positive cells aspirated with the recording pipette. Right lane, molecular weights marker.

(D) Left, V_m and R_{input} plotted over time in 30 s bins during changes in extracellular glucose concentration, in the presence or absence of synaptic inhibitors. Right, representative voltage traces at 5mM (black) to 0.5mM (blue) glucose showing the response to the hyperpolarizing current steps (sketched below traces) applied to monitor R_{input} . See also Figure S1.

(E) Glucose effect on V_m and R_{input} , in the presence (n=13) or absence (n=12) of synaptic inhibitors.

(F) Left, representative voltage traces at 5mM (black) and 0.5mM (blue) glucose showing action potential trains elicited by a depolarizing current injection (below). Right, FI curves (n=10) obtained at 5mM (black) and 0.5mM glucose (blue).

(G) Glucose effect on rheobase (n=12) and FI curve gain (n=10), in the presence or absence of synaptic inhibitors.

(H) Changes in membrane potential, input resistance, rheobase, and FI curve gain as a function of glucose concentration (n=5). Dashed lines are monoexponential decay fits to the data.

Figure 2. Biophysical Mechanisms of the Glucose-Inhibited Effect

(A) Left, current-voltage plot showing a reversible inward shift when switching from 5 to 0.5 mM glucose. Middle, the current-voltage plot of net glucose-induced current (n=12) shows an

outward rectification fitted by the GHK current equation (red dashed line). Right, time course of net glucose-induced current in response to voltage steps (below). See also Figure S2.

(B) Voltage trace recorded with high Cl^- intracellular solution showing a depolarizing response to low glucose.

(C) Current trace recorded at -70mV with high Cl^- intracellular solution and in the presence of TTX showing a glucose-induced outward K^+ current.

(D) Glucose effect on V_m ($n=11$), R_{input} ($n=11$), rheobase ($n=9$) and FI curve gain ($n=9$) with high Cl^- intracellular solution.

(E) Voltage trace showing the depolarization induced by quinine and its blocking effect on the response to changes in glucose concentration.

(F) Quinine effect on V_m and R_{input} ($n=6$) mimics low glucose and impairs glucose sensing.

Figure 3. Glucose Effect Is Mediated by Cell Metabolism

(A) Voltage trace showing a partly reversible depolarizing effect of 2-DG in the presence of 5mM glucose.

(B) 2-DG effect on V_m and R_{input} ($n=5$) mimics low glucose.

(C) Voltage trace showing a reversible depolarizing effect of D-glucosamine in the presence of 5mM glucose.

(D) D-glucosamine effect on V_m and R_{input} ($n=7$) mimics low glucose.

(E) Voltage trace showing the response to extracellular glucose when the cell was recorded with a glucose-containing intracellular solution (upper trace). In the same cell, adding D-glucosamine to the bath induced a depolarization and an increase in R_{input} (lower trace).

(F) Intracellular glucose infusion blunts V_m and R_{input} responses to glucoprivation, an effect reversed by D-glucosamine ($n=7$).

Figure 4. Glucose Effect Depends on AMPKinase Activation

- (A) Voltage trace showing a partly reversible depolarizing effect of oligomycin in the presence of 5mM glucose.
- (B) Oligomycin effect on V_m and R_{input} (n=7) mimics low glucose.
- (C) Voltage trace showing a depolarizing effect of AICAR in the presence of 5mM glucose.
- (D) AICAR effect on V_m and R_{input} (n=7) mimics low glucose.
- (E) Voltage trace showing the blocking effect of compound C on the depolarization induced by low glucose.
- (F) Compound C inhibits V_m and R_{input} (n=7) responses to low glucose.
- (G) Confocal images of brainstem sections showing the colocalization of AMPK subunit pAMPK α immunostaining (green) with tdTomato labeling of Glut2 neurons (red, arrows).

Figure 5. NTS Glut2 Neurons Are GABAergic Cells Projecting to DMNX

- (A-B) Confocal images of brainstem sections showing the colocalization of GABAergic neuron marker GAD67 and inhibitory neuron marker parvalbumin (PV) immunostainings (green) with tdTomato labeling of Glut2 neurons (red, arrows).
- (C) Left, projection image of a confocal stack of a tdTomato-positive neuron (red, star) patched in NTS with a pipette solution containing biocytin. Neutravidin labeling (green) reveals the path of the biocytin-filled axon (arrowheads) towards DMNX, which contains ChAT immunopositive neurons (purple). Right, 3D rendering of a high resolution image of the area delineated with a white dashed line in the left panel, showing axonal boutons in DMNX.

Figure 6. Optogenetic Stimulation of Glut2 Neurons

- (A) IR-DIC and fluorescence image (EYFP) of a Glut2 neuron in the NTS. Scale bar, 10 μ m.
- (B) Example firing response (current clamp) and photocurrent (voltage clamp) induced by continuous blue light illumination (473 nm).
- (C) Example photocurrents induced by brief pulses (10ms) of blue light of increasing frequencies.

(D) Schematic representation of the recording configuration during *in vivo* optogenetic stimulation.

(E) Vagal firing rate in response to pulsed blue light stimulation (dotted blue line) in ChR2-expressing mice and their control littermates.

(F) Blood glucagon levels measured at baseline and at the end the optogenetic stimulation in both mice groups.

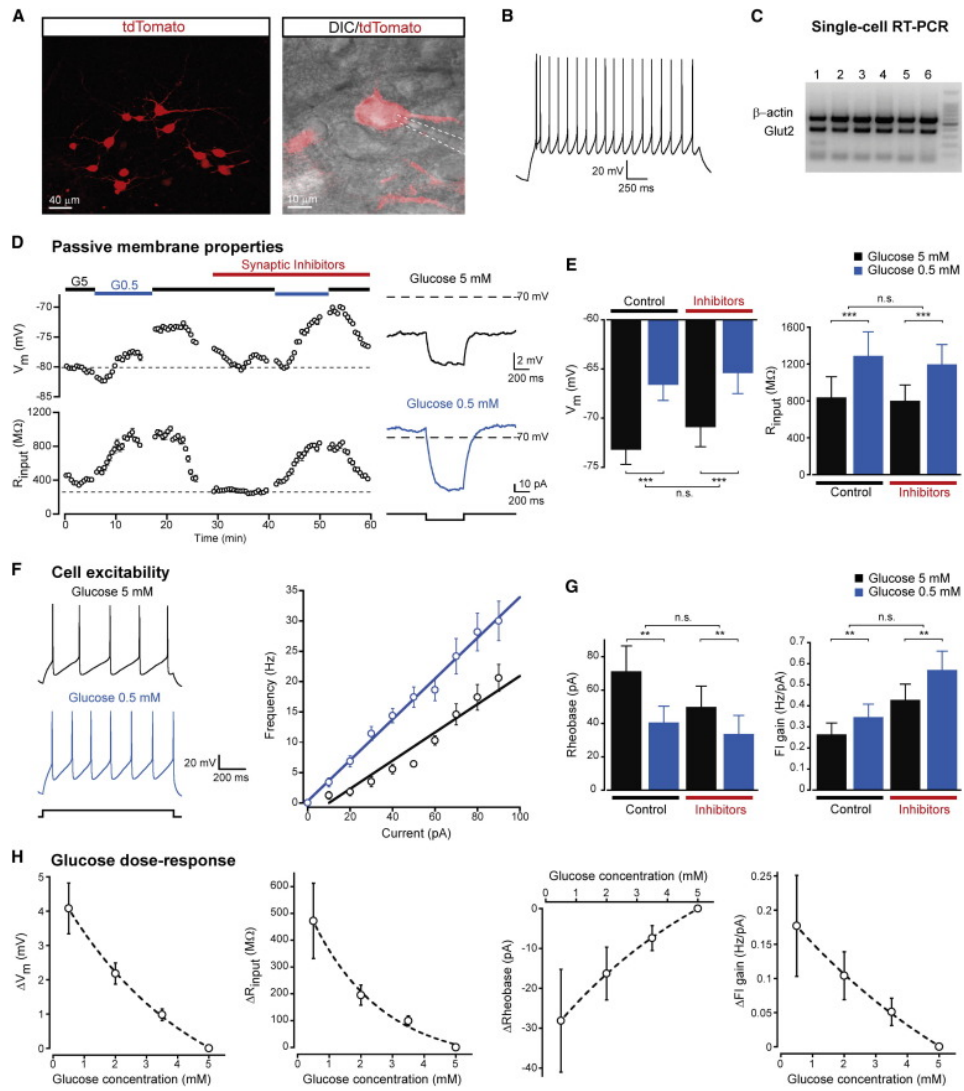


Figure 1

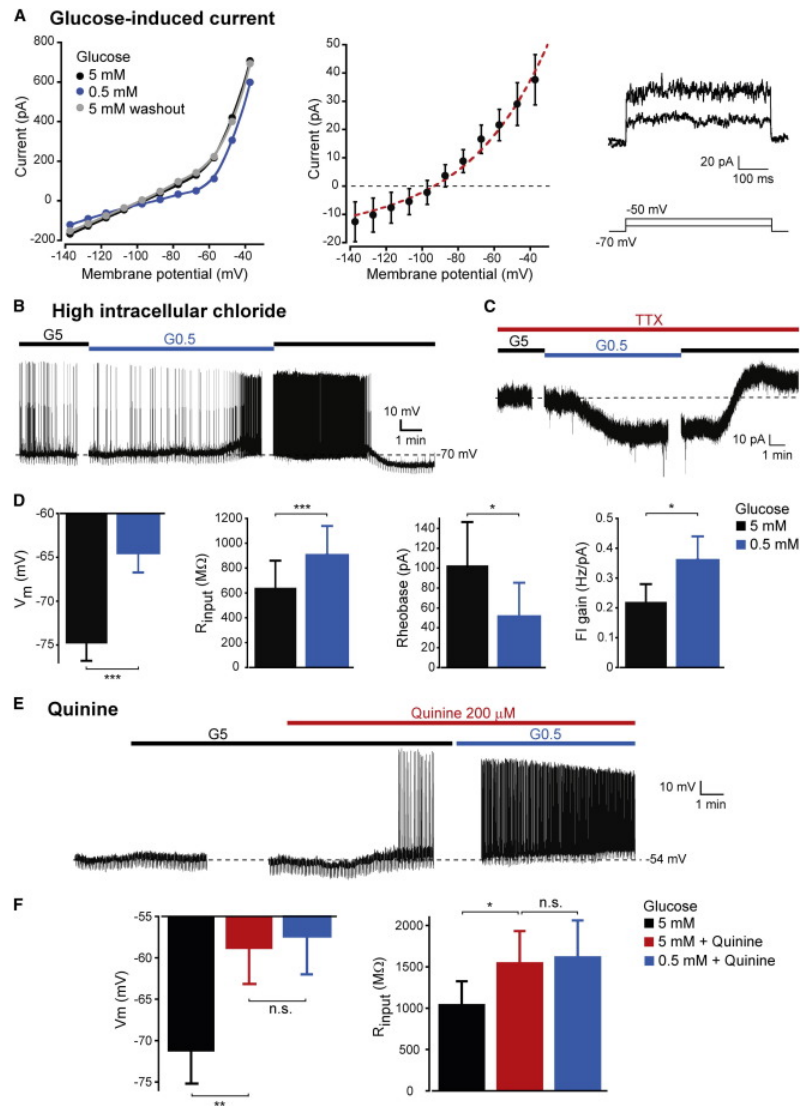


Figure 2

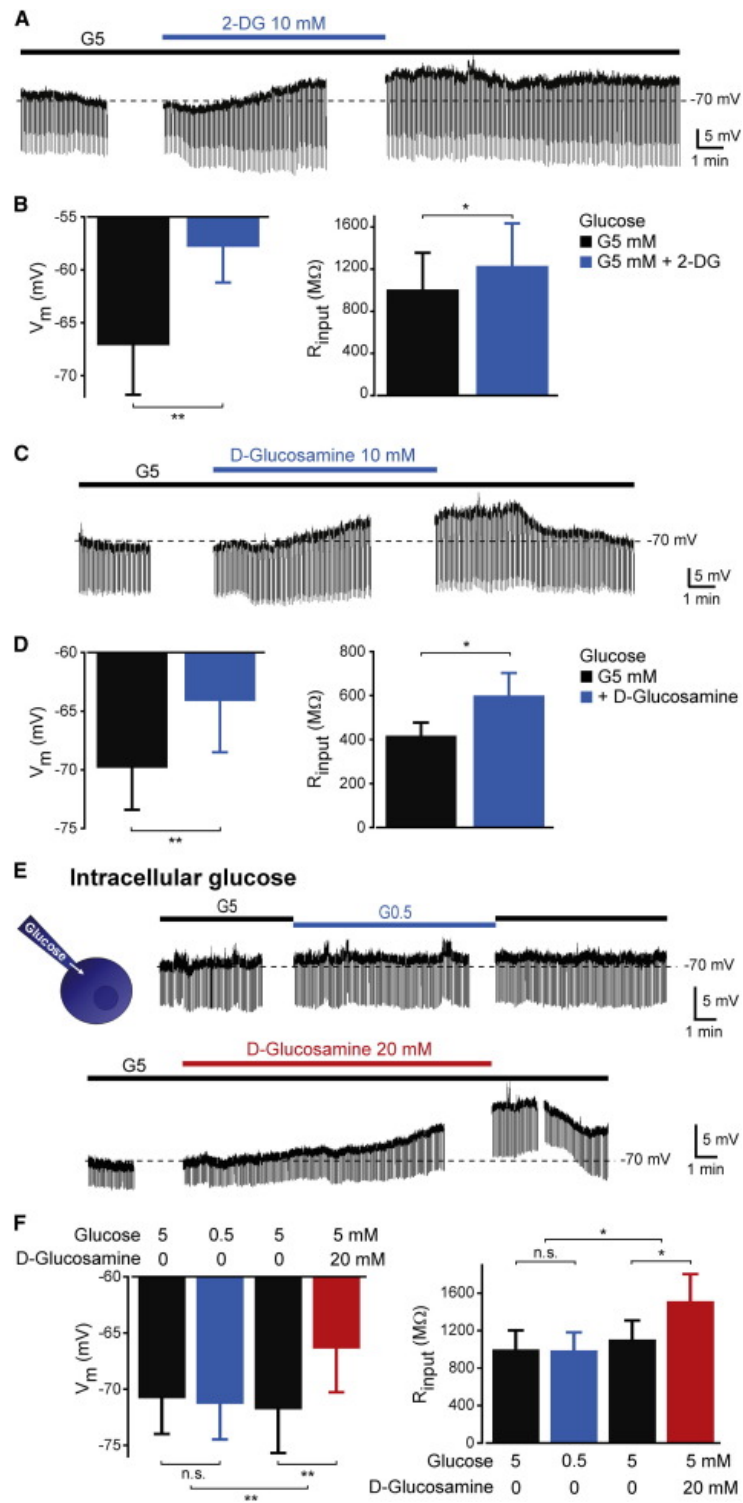


Figure 3

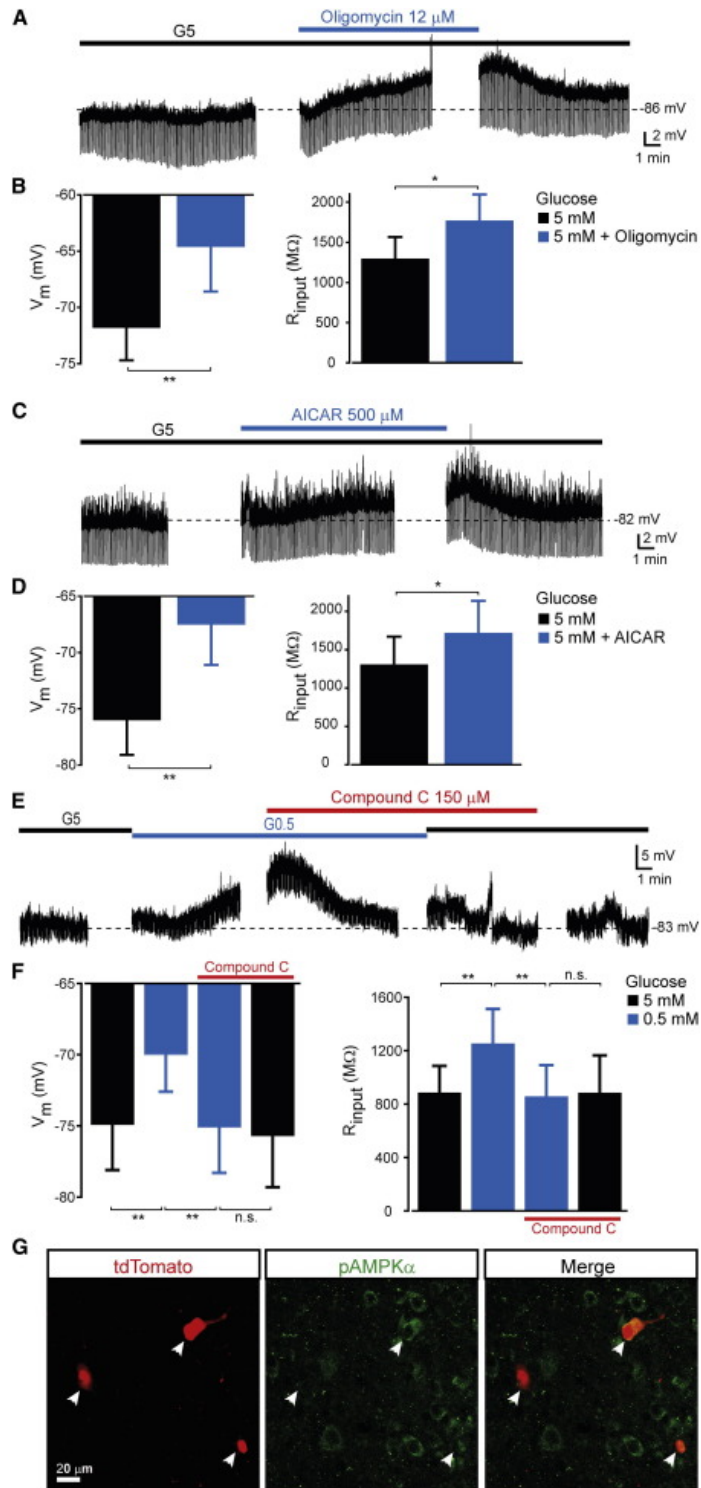


Figure 4

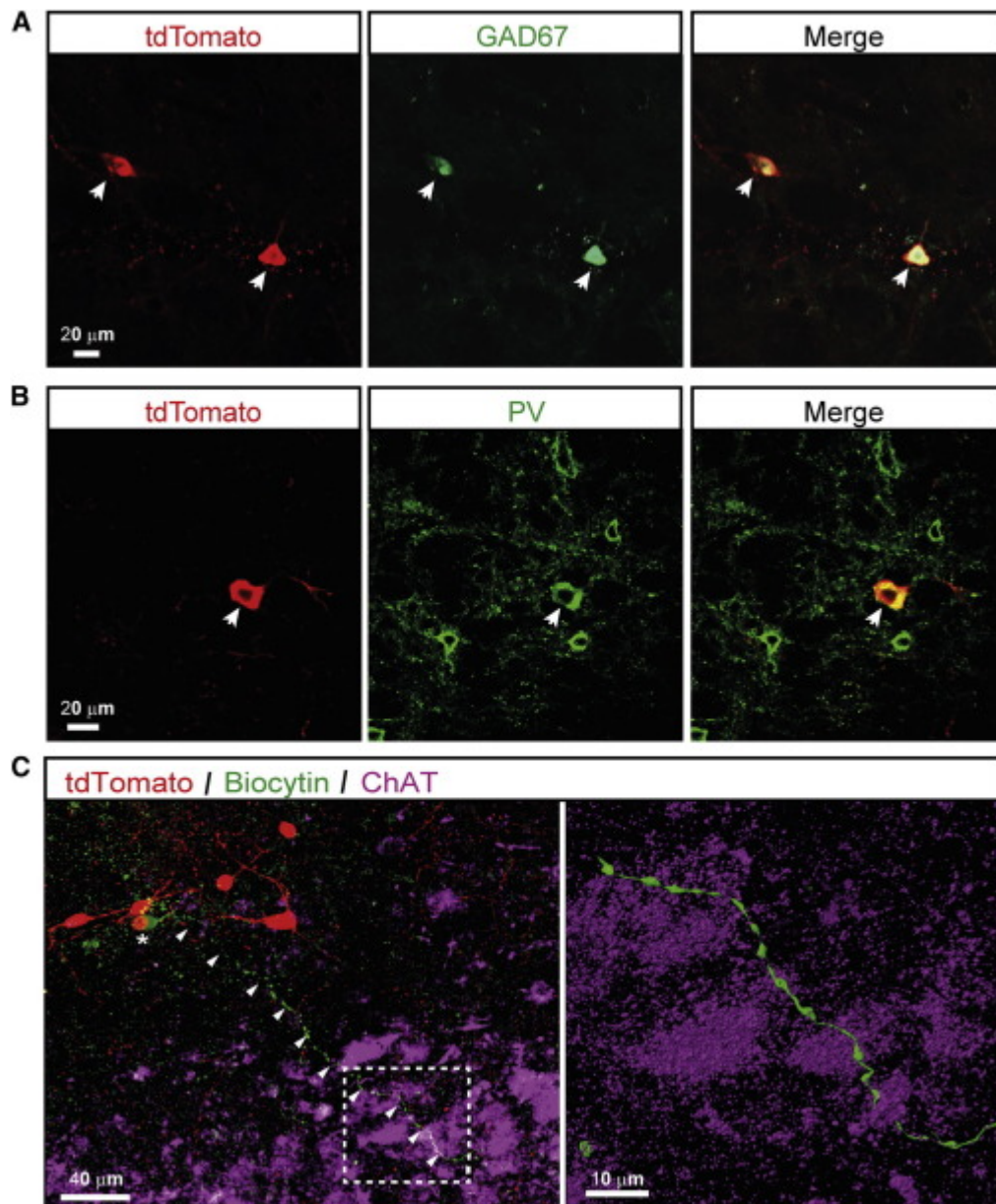


Figure 5

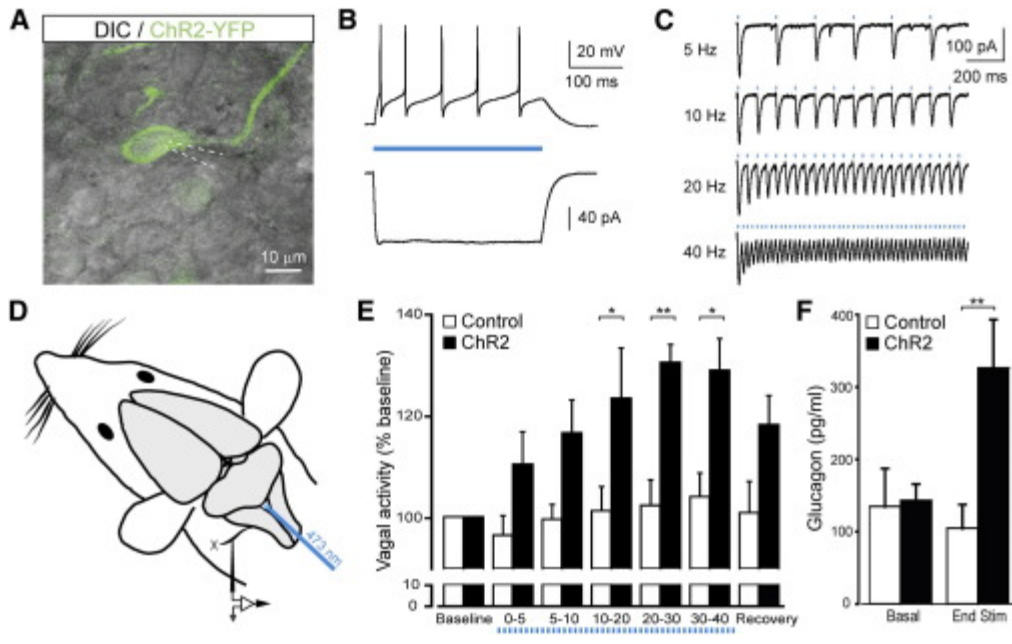


Figure 6